Numerical tools for musical instruments acoustics: analysing nonlinear physical models using continuation of periodic solutions

Sami Karkar, Christophe Vergez, Bruno Cochelin

ACOUSTICS 2012

Numerical tools for musical instruments acoustics: analysing nonlinear physical models using continuation of periodic solutions

S. Karkar, C. Vergez and B. Cochelin

LMA – CNRS (UPR 7051) / Aix-Marseille University, 31, chemin J. Aiguier, 13402 Marseille Cedex 20, France
karkar@lma.cnrs-mrs.fr

We propose a new approach based on numerical continuation and bifurcation analysis for the study of physical models of instruments that produce self-sustained oscillations. Several physical models (clarinet and saxophone) are formulated as nonlinear dynamical systems, whose periodic solutions are directly obtained using the harmonic balance method. This method yields a set of nonlinear algebraic equations. The solution of this system, which represent a periodic solution of the instrument, is then followed using a numerical continuation tool when a control parameter (e.g. the blowing pressure) varies. This approach enables us to compute the whole periodic regime of the instruments, without any additional simplification of the models, thus giving access to characteristics such as playing frequency, sound level, as well as sound spectrum as a functions of the blowing pressure or bow velocity. Finally, we show how the same approach can be used to study the oscillation threshold.

1 Introduction

While system dynamicists are used to bifurcation analysis and numerical continuation tools, the musical instrument acousticians often use numerical integration or other simulation tools to investigate their physical models. In this paper, we propose a general method for analysing the dynamical properties of self-sustained musical instruments using traditional numerical techniques such as the harmonic balance technique associated with numerical continuation tools. In a previous conference paper [1], the authors presented a single-reed woodwind instrument model as well as the numerical methods (spectral and continuation methods). In this paper, we first analyse the effect of the beats of the reed against the mouthpiece and present an alternative model, in which the contact itself is not rendered, but the effect of the closure of the reed channel is rendered (section 2). Then, we show how our approach is suited to real instruments whose input impedance has been measured, and how it thus applies to conical bores (section 3). Finally, we show how the same approach can be used to study the evolution of particular points, like the oscillation threshold (section 4).

2 The clarinet

2.1 Model

The physical model is split into a linear element and a nonlinear coupling element.

2.1.1 Linear part

For single reed woodwind instruments, there is actually two linear parts : the air column, that constitutes the acoustical resonator, and the reed –a mechanical oscillator.

The first one is characterized by its impedance $Z(\omega)$ in the frequency domain:

$$Z(\omega) = P(\omega)/U(\omega),$$

where P is the acoustical pressure and U the acoustical volume flow at the input end of the resonator.

Whether known analytically, numerically, or experimentally trough measurements, the input impedance of the resonator can be decomposed as a sum of linear, "complex modes", as used in [2]:

$$Z(\omega) = Z_c \sum_{n=1}^{\infty} \frac{C_n}{j\omega - s_n} + \frac{C_n^*}{j\omega - s_n^*} \tag{1}$$

where the C_n, s_n are complex coefficients, the * sign denotes the complex conjugate, and $Z_c = \rho c/S$ is the characteristic impedance. Note that the imaginary part of the poles s_n is related to the resonance frequencies, that is, the frequencies of the peaks of $|Z|$.

Thus, denoting P_n each mode of pressure, and keeping only the first N_m modes, one gets the following complex, ordinary differential equations:

$$P_n' = Z_c C_n U + s_n P_n \quad , n = 1..N_m \tag{2}$$

$$P = \sum_{n=1}^{N_m} (P_n + P_n^*) \tag{3}$$

The second linear part is the reed: the reed oscillations are driven by the pressure difference across its faces, and the frequency response of this system typically shows several resonances, the first of which is usually well beyond playing frequencies. Thus, a single mechanical mode (the first bending mode) is supposed to be needed to account for the dynamics of the reed and, denoting h the dimensionless height of the reed channel, one gets:

$$h''(t) = -q_r \omega_r h'(t) - \omega_r^2 (h(t) - h_0) - \frac{\omega_r^2}{K} S_r \Delta P + F_c \tag{4}$$

where $\Delta P = P_m - P$ is the difference between the mouth pressure and the pressure inside the mouthpiece, K is the stiffness of the reed, S_r the effective area of the reed, h_0 is the reed channel height at rest, ω_r is the angular frequency of the reed mechanical mode, and q_r is the modal damping. The contact force F_c is a regularisation of the unilateral contact condition $0 < F_{uc} \perp x > 0$:

$$F_c = \epsilon F_0 \left(\frac{h(t)}{h_0} \right)^{-2} \tag{5}$$

where $\epsilon << 1$ is the regularisation parameter and $F_0 = K h_0$ is the scaling factor.

2.1.2 Nonlinear coupling

The nonlinear coupling typically involves a nonlinear algebraic equation which is easier to use in the time domain. However, as it has been shown in [3], a purely frequency-based formulation of an arbitrary high-order harmonic balance can be easily achieved if the nonlinearity is quadratic. The authors also showed that a lot of nonlinearities can be recast into quadratic extended systems using additional variables. Let us illustrate this on our single reed woodwind model.

In the case of single reed woodwinds, the acoustical volume flow that enters through the reed channel is:

$$U(t) = W h(t) V(t), \tag{6}$$

where W is the width of the reed channel, $h(t)$ its height, and $V(t)$ the mean jet velocity, which is defined (see [4]) as:

$$V(t) = \text{sign}(\Delta P(t)) \sqrt{2|\Delta P(t)|/\rho}. \tag{7}$$

2.1.3 Dimensionless model

Dimensionless variables and parameters are defined as follows:

- $P_M = K_r h_0$ is the static reed channel closure pressure,
- $\zeta = Z_c W h_0 \sqrt{2/\rho P_M}$ is the flow scaling parameter,
- $u = U Z_c / P_M$ is the dimensionless volume flow,
- $p = P/P_M$ is the dimensionless mouthpiece pressure,
- $p_n = P_n/P_M$ is the dimensionless n-th pressure mode,
- $\gamma = P_m/P_M$ is the dimensionless mouth (or blowing) pressure,
- $x = h/h_0$ is the dimensionless reed channel height,
- $v = V/\sqrt{2P_M/\rho}$ is the dimensionless jet velocity,
- $f = F/F_0$ is he dimensionless regularised contact force.

The complete, dimensionless model then reads:

$$p_n' = s_n p_n + C_n u, \quad n = 1..N_m \tag{8}$$

$$p = 2 \sum_{n=1}^{N_m} \mathcal{R}\mathrm{e}(p_n) \tag{9}$$

$$\frac{1}{\omega_r} x' = y \tag{10}$$

$$\frac{1}{\omega_r} y' = 1 - x - q_r y + p - \gamma + f \tag{11}$$

$$f = \epsilon / x^2 \tag{12}$$

$$u = \zeta x v \tag{13}$$

$$v = \mathrm{sign}(\gamma - p)\sqrt{|\gamma - p|} \tag{14}$$

2.1.4 Model parameters

Air physical properties: the air temperature is $T = 25°C$, its volume mass is $\rho = 1.185\mathrm{kg/m}^3$, and the sound speed is $c = 346.1\mathrm{m/s}$.

Reed mechanical properties: the reed resonance frequency is $\omega_r = 2\pi.1500\mathrm{Hz}$, its modal damping is $q_r = 1$, the reed stiffness is $K = 8.10^6\mathrm{N/m}^3$.

Control parameters: the parameter that reflects the control of the player on his lip and the mouthpiece-reed system is $\zeta = 0.318$, and the (dimensionless) blowing pressure γ is let as a free parameter for the continuation.

Regularization parameter: $\epsilon = 1.10^{-4}$.

The resonator is a cylinder of length L=57cm and radius r=7mm, whose input impedance is analytically computed taking into account the radiation impedance at the output end as well as visco-thermal losses along the pipe, as given by [2]. The coefficients of the complex modal decomposition are computed using the MOREESC software [5], up to twelve modes.

2.2 First periodic regime

The static regime of this model (not shown) presents a series of Hopf bifurcations. The first one destabilizes the static regime and is the starting point for a first branch of (locally stable) periodic solutions: it is the oscillation threshold, located at $\gamma_{th} = 0.376$. The frequency of the emerging oscillations is close to the first resonance frequency of the bore: this regime corresponds to the first register of the instrument. Figure 1 illustrates this periodic branch: the first harmonic's cosine coefficient the mouthpiece pressure $p_{c,1}$ is plotted as a function of the blowing pressure γ. It was computed with the harmonic balance method (H=50 harmonics), together with the ANM continuation technique (series order: 20), using the MANLAB software [6].

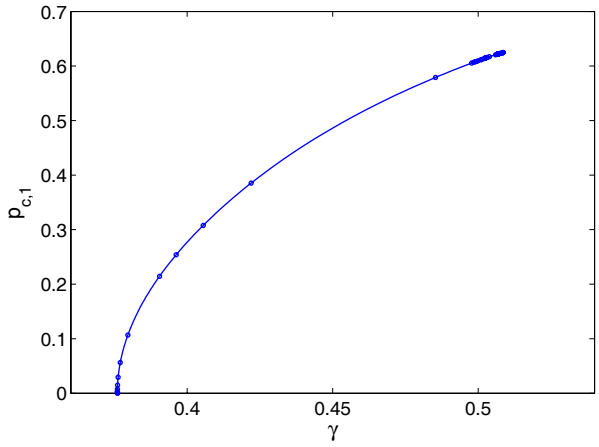

Figure 1: First periodic regime of the clarinet: the curve represents the branch of periodic solutions that destabilizes the static regime at the oscillation threshold ($\gamma_{\mathrm{th}} = 0.373$). Computed using ANM (power series order: 20) and HBM (50 harmonics). (—) : first harmonic's cosine coefficient of the pressure $p_{c,1}$ as a function of the blowing pressure γ. The circles mark the beginning of each continuation step.

2.2.1 Multiple rebounds of the reed

The continuation steps show an accumulation near $\gamma = 0.5$, very close to the beating threshold, that is to say the point of the branch where the periodic solutions have grown large enough for the reed to touch the mouthpiece during the period. Eventually, the continuation seems to stop there, while the branch does not stop there. This is directly due to the contact between the reed and the mouthpiece, which is a crucial point of the model. However, here, something clearly prevents the continuation from proceeding normally. To understand why, we selected a few solutions very close to each other, in that region of the branch.

A close look to the beats (fig.2) reveals the complexity of the movement, and explains why the continuation fails: the modelling of the contact involves the computation of each individual rebound of the reed on the mouthpiece lay, while the size and the number of these rebounds can change a lot for very close values of γ.

These individual bounds are essentially due to the form of our contact force and are not necessarily physically based (at least in in their size, form and number). Thus, such a fine resolution concerning the beating phenomenon is not necessary and, in our case, is actually harmful to the continuation process.

Note that the same problem occurs when using a collocation-based continuation tool (such as the AUTO software [7]), as the collocation method is subject to the same rebound-resolution constraints. One can increase the resolution to the level needed (as we actually did for this figure) and eventually the continuation can (sometimes) proceed and com-

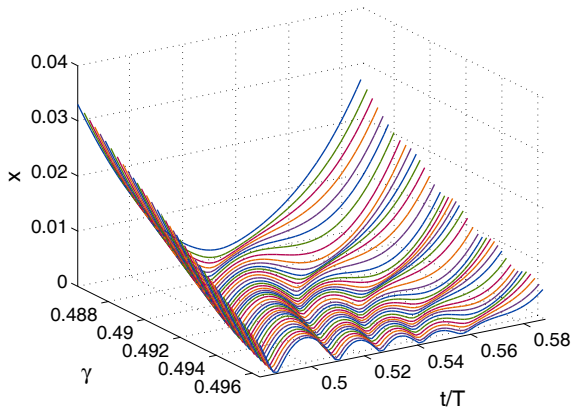

Figure 2: A few periodic solutions on the branch near $\gamma = 0.48$: zoom on the part of the period where the beating occurs. Each curve shows the time series of the reed position x. Computed with HBM using 300 harmonics on a simplified model with a single acoustic mode.

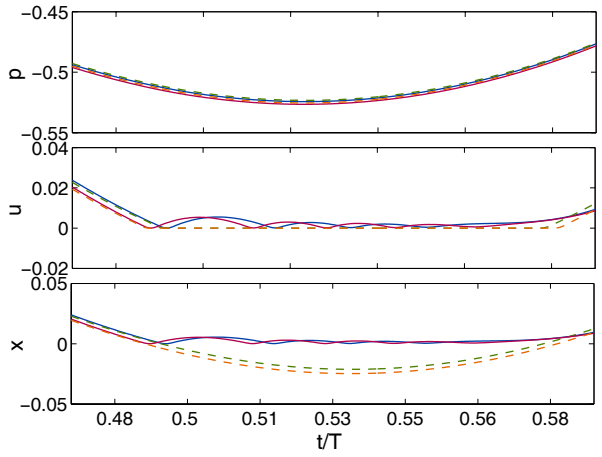

Figure 3: Comparison between a model with regularised contact (—) and a model with a phantom reed (- - -): partial time series of the mouthpiece pressure p, the volume flow u entering the reed channel, and the reed tip position x when the beating occurs. corresponding values of γ are between 0.494 and 0.496.

pute the whole branch, however the steps are so short that the main advantage of the continuation method (providing a piecewise-continuous representation of the branch) is discarded.

2.2.2 The "phantom" reed

A crude, but often used approximation in sound synthesis (see for instance [8]) for modelling the contact of the reed and the mouthpiece is that of a "phantom" reed that can move through the mouthpiece as if it were not present, but the reed channel height in the volume flow equation is set to zero if it becomes negative. Put otherwise, the modified equations of the model are:

$$F_c = 0 \tag{15}$$

$$U(t) = Wh^+(t)V(t), \tag{16}$$

where $h^+(t)$ denotes the positive part of $h(t)$.

This approximation is equivalent to a reed that would instantaneously stop when it touches the mouthpiece, when the pressure drop is negative, and instantaneously go back with a prescribed velocity when the pressure drop becomes positive again. Because the reed is not exactly in phase with the pressure variations, it is not correct. However, the effect of this approximation remains to be quantified. To this end, we compared the effect of this approximation on the periodic solutions of our clarinet model, with a very fine time resolution, just after the beating threshold (same conditions as fig.2).

The results are shown figure 3: we plotted $p(t)$, $u(t)$ and $x(t)$ of several periodic solutions for very close values of γ near the beating threshold. On the left plot are displayed the results for the model that contains the regularised contact force, while on the right plot are displayed the results for the approximation. For $\gamma = 0.5$, the norm-2 of the relative difference on $p(t)$ as well as on $u(t)$ is less than 1.10^{-4}, while the relative difference on the value of the period is of the same order of magnitude. Thus, we are now confident that this approximation is justified.

2.2.3 Stability of the first periodic branch

Using this new formulation, the continuation is much more fluent and enables to compute the whole periodic branch, as shown figure 4.

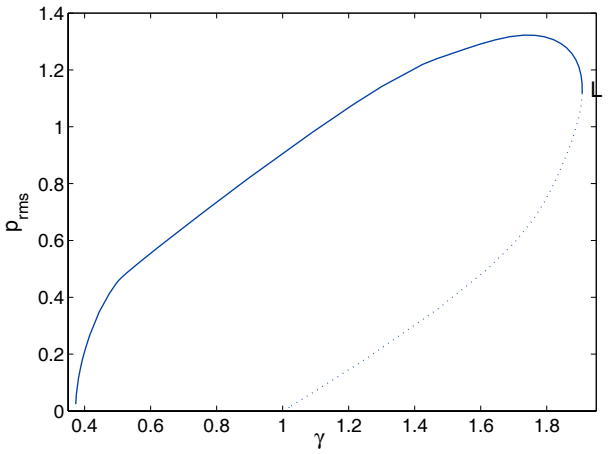

Figure 4: Stability of the first periodic branch of the clarinet: RMS value of the mouthpiece pressure vs. the blowing pressure γ. (—) stable parts, $(\cdots)$ unstable parts.

The stability was assessed using a linear stability analysis based on a Hill algorithm (see [9]), integrated to the software.

Several characteristic properties of this clarinet dynamics can be retrieved from this diagram. The left-most point of the curve marks the oscillation threshold, located at $\gamma_{\text{th}} = 0.373$. The maximum value of the RMS mouthpiece pressure, that is to say the saturation threshold, is $p_{\text{sat}} = 1.33$, revealing the dynamic range of the clarinet for this note[1], located at $\gamma_{\text{sat}} = 1.74$. Finally, the limit point (denoted 'L' on the figure) marks the extinction threshold (for increasing γ) and is located at $\gamma_{\text{ext}} = 1.91$.

Fig.5 shows the evolution of each harmonics amplitude as a function of the blowing pressure. It should be noted that the "Worman rule", stating that near the oscillation threshold,

[1] And for this particular set of parameters, only.

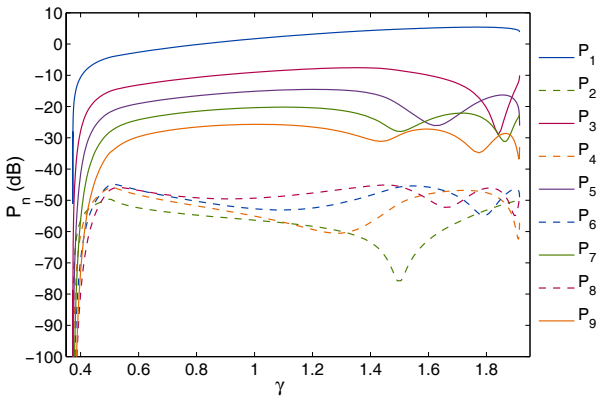

Figure 5: Evolution of the harmonics amplitude along the stable part of the first regime.

the n-th harmonic amplitude P_n should vary as P_1^n, is verified up to $\gamma = 0.39$, which highlights the very limited range of validity of this analytical formula for the spectrum.

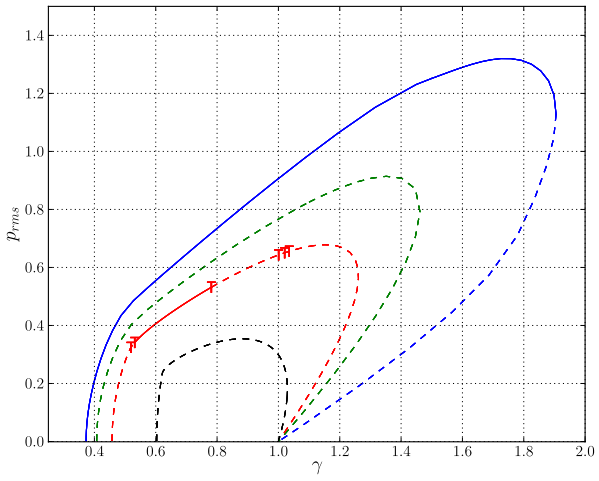

Figure 6: Bifurcation diagram: periodic regimes of the clarinet. Each curve represents a branch of periodic solutions. Plain lines denote stable parts, and unstable ones are denoted by a dotted line. Computed using the AUTO software.

Other periodic regimes Three other periodic regimes exist, due to the three other Hopf bifurcations on the static regime. The static regime being unstable on both sides of these bifurcations, these regimes cannot be attained in practice from the static regime. However, to check if these periodic branches are stable or not, one needs to compute it entirely.

Fig.6 shows the whole bifurcation diagram with the four periodic branches. As the bifurcation diagram clearly shows, there is only one other stable part, on the third periodic branch ($f \simeq 5f_0$), which might be connected to the first one by a branch of bi-periodic solutions (yet to find and to compute...), as suggest the torus bifurcations that are detected.

Therefore we conclude that the player would be able to play, at least, the first regime on its entire dynamic range, in this configuration (with all tone holes closed and the given values of the model parameters, see 2.1.4).

3 Application to conical instruments

We now illustrate two applications of the method, using the same model: application to conical single-reed instruments such as saxophones, and the use of a measured impedance on a real instrument.

3.1 Using a measured impedance

Instead of using an analytical model of a cylindrical bore (or whatever geometry), one might want to use the measured impedance of a real instrument. One "simply" has to compute the coefficients of the modal representation (1) of this measured impedance, by a nonlinear fit. In the present case, we use the measured impedance of the lowest key of an alto saxophone. Note that even though the measure, limited to the 20-1608Hz range, shows up only 10 peaks, a very good fit is obtained with 11 modes, as shown figure 7.

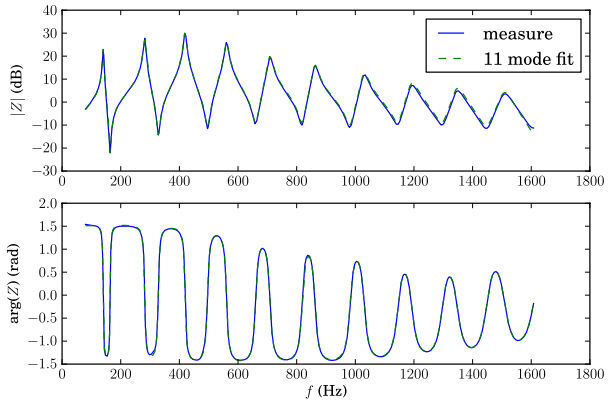

Figure 7: Measured and fitted modal impedance of an alto saxophone (lowest key).

3.2 Model parameters

The only model parameters that have been updated from the previous example are:

- the modal coefficients, determined by curve fitting,
- the reed modal damping $q_r = 2.0$,
- the lip-reed-mouthpiece control parameter $\zeta = 2.5$.

3.3 First periodic regime

Figure 8 shows the beginning of the first periodic regime. With this set of parameters, it corresponds to the first register, and starts with an inverse bifurcation. Thus, the lower part of the curve being unstable, the player cannot play pianissimo, unless he/she changes the control parameter ζ.

Note that the computation of this curve is much more computer intensive than for the clarinet, because of the form of the impedance, which explains why we did not compute the full periodic branch. Note also that these results are much dependant on the quality of the modal fitting of the input impedance. A robust method for this fit seems to be a difficult problem that could need further investigations.

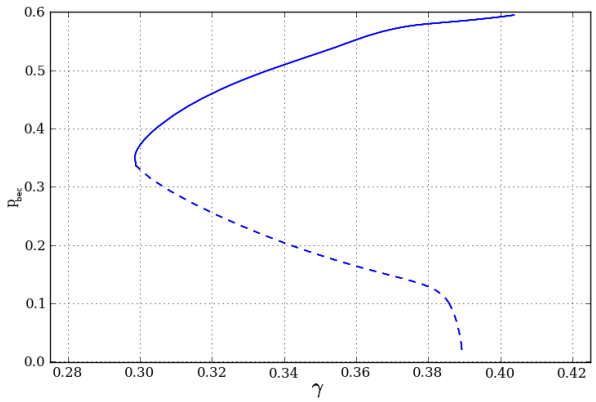

Figure 8: First periodic branch of the saxophone : inverse bifurcation at the start of the branch. Plain lines denote stable parts, and unstable ones are denoted by a dotted line.

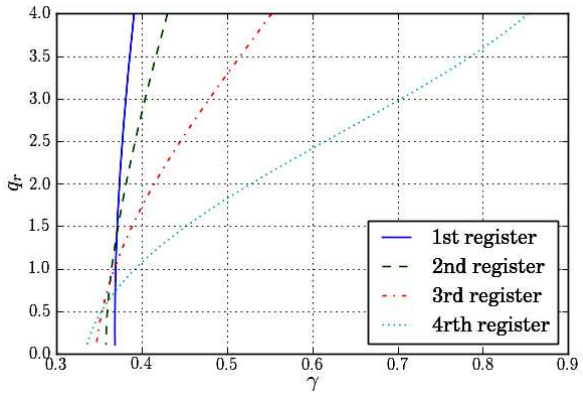

Figure 9: Branches of Hopf bifurcations for the saxophone model. Fixed parameters: $\omega_r = 2\pi$i500, $\zeta = 2.5$.

4 Parametric study of special points

The continuation framework is, by essence, a tool for parametric study. Thus, it is well suited to characterise the evolution of a characteristic point (such as oscillation threshold, saturation threshold, extinction threshold, etc.) when one or several parameters vary. For instance, in [10] the authors showed that the oscillation threshold of the proposed model (whether applied to a saxophone or a clarinet) is characterized by a set of nonlinear equations, which is an extension of the dynamical system's equations, on which a continuation algorithm can be applied with two varying parameters.

As an example, we present an application of this method to study how the reed damping q_r influences the oscillation threshold and the register selection.

4.1 Effect of the reed damping

We use the previous model of a saxophone, using the measured impedance fitted with 11 modes.

From the static solution with q_r=4, ζ=2.5, and γ=1.2 (the reed channel is closed, so an analytical solution is trivial), we used the classical continuation with H=0 and stability analysis to compute the corresponding branch of static solutions and detect the Hopf bifurcations: there are four of them, the first[2] of which is the oscillation threshold. Moreover, the associated frequency of that bifurcation indicates the frequency of the emerging oscillations which allows us to determine the selected register[3].

Then, for each of the possible registers, we applied the continuation method to the extended system defining the Hopf bifurcation to obtain the branch of Hopf bifurcation. These branches are plotted fig.9: for a given value of q_r, the selected register is the one corresponding to the left-most curve. This shows how the reed damping is a crucial parameter for the selection of the playing register.

5 Conclusion

In this paper, we proposed a general approach for the study of self-sustained reed musical instruments: numerical continuation. We showed the pertinence of this method for the study of permanent regime, the extraction of general dynamical features, as well as the parametric study of characteristics such as the oscillation threshold. We also showed how it can be applied to a real resonator, using a measured impedance.

We would like to emphasize the benefits of this approach for the comparison between models, and point out its possible use to assess the importance of the acoustic flow induced by the reed vibrations, which was neglected in this study.

Recent works [11] have shown that this approach is also suited for the study of a physical model of violin, provided one use a regularized friction function.

Finally, one of the possible extensions to this work is the use of a measured characteristics of the reed, allowing one to get one step closer to an experimental set-up and eventually compare numerical with experimental data.

[2] For an increasing value of γ

[3] In the case of a direct bifurcation only. However, the registers have sufficiently different frequencies so that in the case of an indirect bifurcation, the associated frequency still indicates the selected register.

Acknowledgements

Many thanks to P.Guillemain, J.Kergomard and F.Silva for fruitful discussions on the subject.

References

[1] Sami Karkar, Christophe Vergez, and Bruno Cochelin. Toward the systematic investigation of periodic solutions in single reed woodwind instruments. In *Proceedings of the 20th International Symposium on Music Acoustics (Associated Meeting of the International Congress on Acoustics)*. International Commission for Acoustics, August 2010.

[2] Fabrice Silva. *Emergence des auto-oscillations dans un instrument de musique à anche simple (Sound production in single reed woodwind instruments)*. PhD thesis, Aix-Marseille University, LMA - CNRS, 2009.

[3] Bruno Cochelin and Christophe Vergez. A high order purely frequency-based harmonic balance formulation for continuation of periodic solutions. *Journal of Sound and Vibration*, 324:243–262, 2009.

[4] A. Hirschberg. *Mechanics of Musical Instruments*, chapter 7, pages 291–369. Number 355 in CISM

Courses and Lectures. Springer, Wien - New York, 1995.

[5] Fabrice Silva. Moreesc, modal resonator-reed interaction simulation code, 2009. (last viewed 3/16/2011).

[6] Sami Karkar, Rémy Arquier, Bruno Cochelin, Christophe Vergez, Arnaud Lazarus, and Olivier Thomas. *MANLAB 2.0, an interactive continuation software*, 2010. (last visited 28/06/2011).

[7] E. J. Doedel and B. E. Oldeman. *AUTO-07P : Continuation and Bifurcation Software for Ordinary Differential Equations*. Concordia University, Montreal, Canada, January 2009. (last visited 28 feb. 2012).

[8] Philippe Guillemain, Jean Kergomard, and Thierry Voinier. Real-time synthesis of clarinet-like instruments using digital impedance models. *Journal of the Acoustical Society of America*, 118(1):483–494, 2005.

[9] A. Lazarus and O. Thomas. A harmonic-based method for computing the stability of periodic solutions of dynamical systems. *Comptes Rendus de Mécanique*, 338:510–517, 2010.

[10] Sami Karkar, Christophe Vergez, and Bruno Cochelin. Oscillation threshold of a clarinet model: a numerical continuation approach. *Journal of the Acoustical Society of America*, 131:698–707, jan 2012.

[11] Sami Karkar. *Numerical methods for nonlinear dynamical systems. Application to self-sustained musical instruments*. PhD thesis, Aix-Marseille Univ.(France), 2012.